An Analytical Loss Model for Magnetic Cores Based on Vector Magnetic Circuit Theory

Chengbo Li, Wei Qin, Xiang Ma, Boyu Zhang, Zheng Wang, *Senior Member, IEEE* and Ming Cheng, *Fellow, IEEE*

***Abstract*- Currently, some empirical formula methods, such as the Steinmetz equation, have been widely used in calculating high-frequency magnetic core loss. Although these methods may provide satisfactory accuracy under some certain conditions, they cannot present clear physical interpretation and fail to account for the origin and variation of losses. In this article, we propose a new analytical model to predict core loss by employing a new magnetic circuit theory, i.e., vector magnetic circuit theory. In addition to reluctance, two new components, i.e., magductance and hysteretance are proposed in the vector magnetic circuit, which are used to describe the eddy-current loss and the hysteresis loss, respectively. Thus, the clear physical significance is available with the proposed loss model. Given the geometrical and physical parameters of cores, the loss can be calculated mathematically. Furthermore, the proposed vector magnetic circuit based modeling method provides a different expression form for core loss, where the coefficients are with explicit physical meanings. Because only the measurement data are available with the competition, we employ the nonlinear fitting and Fourier decomposition to obtain the coefficients in the proposed new loss model. By comparison between the prediction results and the competition data, it has been verified that the proposed model could provide accurate and effective prediction of loss for high-frequency magnetic cores.**

I. Introduction

Accurately predicting magnetic core losses is crucial to achieving optimal design of magnetic components [1]. Currently, there are three main methods used to calculate these losses: Steinmetz equation-based methods, loss separation model, and hysteresis model [2]. The loss separation model with the terms eddy current loss, hysteresis loss, and abnormal loss is primarily based on the G. Bertotti model [3]. On the other hand, the hysteresis model is based on the Preisach and Jiles-Atherton models [4-5], which are difficult to be applied in practical situations and lack universality [6].

For a long time, the empirical formula methods for core loss has been favored by engineers due to its practicality and simplicity [7-11], gradually moving from scientific research to the field of engineering applications. The emerging methods like neural networks are now becoming popular for their higher accuracy [12-14], which are significant in engineering applications. But they are sometimes lack of fundamental physical concepts in the calculation of magnetic core loss [15].

Previously, some researchers have tried to define more magnetic parameters in addition to reluctance, in order to model the characteristics of magnetic circuits such as losses more clearly [16-18]. However, almost all of them defined the magnetic parameters based on the duality between electrical circuit and magnetic circuit. Thus, those defined magnetic parameters are lack of the physical properties of magnetic circuit. For example, the "transference" parameter in the Laithwaite magnetic circuit model [19] is solely mathematically dual to the inductance in the electrical circuit. Consequently, it is hard to use the "transference" concept to clearly describe some physical characteristics, e.g., power losses in magnetic circuit. Besides, the article of [19] also fails to characterize phase angle of magnetic flux in electro-magnetic devices like transformers and electric machines.

Recently, Prof. Cheng's team from Southeast University proposed a new vector magnetic circuit theory [20-21], which merges the magnetic circuit and electromagnetic field theories, introducing a vector magnetic circuit model. Different from the previous scalar magnetic circuit with only reluctance, this new model comprises three components, i.e., reluctance, magductance, and hysteretance. The model enables a deeper understanding of the characteristics and physical significance of magductance and hysteretance components, as well as the magnetoelectric power law. The theory attempts to explain the origins of eddy current loss, hysteresis loss, and the phase shift between magnetomotive force and magnetic flux within the magnetic circuit. On this basis, this article first recalls the concept of vector magnetic circuit, then presents the analytical loss model for magnetic circuit, demonstrates the application process in the loss calculation of magnetic core. Finally, we verify these methods using competition data of materials 3E6 and N87.

II. Vector Magnetic Circuit Theory

Consistent with traditional scalar magnetic circuit theory, the reluctance, expressed by $\mathcal{R}$, represents the obstruction effect that magnetic fluxes encounter when they pass through a magnetic circuit. The formula of reluctance is as follows:

$$\mathcal{R} = \frac{l}{\mu S} \tag{1}$$

where μ is the magnetic permeability.

Based on the obstructing effect of a closed conductive coil on the alternating magnetic flux [20], the magductance has been defined as follows:

$$\mathcal{L} = \frac{\Gamma}{\Phi} = \frac{NQ}{\Phi} \tag{2}$$

where Γ is the charge linkage in N turns of closed conductive coil. N is the turns number of the coil. Q is the moving charge. Φ is the magnetic flux of magnetic circuit. The terminal characteristic of $\mathcal{L}$ can be expressed as:

$$\mathcal{F}_{\mathcal{L}} = \mathcal{L}\frac{\mathrm{d}\Phi}{\mathrm{d}t} \tag{3}$$

where $\mathcal{F}_{\mathcal{L}}$ is the magnetomotive force (MMF) of magductance component. The magductance could essentially represent the eddy-current effect in magnetic materials.

Based on the magductance component, we constructed the vector magnetic circuit theory and proposed the magnetoelectric power law in [20], which could be used to solve the long-standing problem to calculate the power of electromagnetic equipment through magnetic circuit directly. Recently, our team have further proposed the concept of hysteretance besides the magductance [21]. It could essentially represent the hysteresis effect in magnetic materials under alternating magnetic flux. The hysteretance can be defined as:

$$C = -\frac{\int \Phi \mathrm{d}t}{\mathcal{F}_C} \tag{4}$$

where $\mathcal{F}_C$ represents the MMF on the hysteretance component.

The unit of hysteretance C is Wb·s/A, and its terminal characteristic is given as follows:

$$\mathcal{F}_C = -\frac{1}{C}\int \Phi \,\mathrm{d}t \tag{5}$$

Fig. 1 shows the complete vector magnetic circuit proposed by our team, which comprises three fundamental passive components, namely reluctance, magductance, and hysteretance.

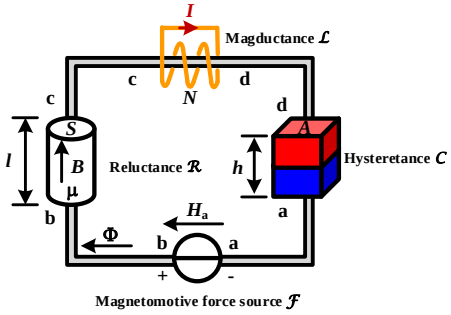

Fig. 1 Reluctance $\mathcal{R}$, magductance $\mathcal{L}$ and hysteretance C are connected in series

III. Analytical Loss Model for Magnetic Core

We use the magnetic circuit to evaluate the power loss in magnetic core. When the magnetic circuit is excited by a steady-state sinusoidal magnetic electromotive force, the following steady-state expression can be obtained using the phasor method:

$$\dot{\mathcal{F}} = \mathcal{R}\dot{\Phi} + \mathrm{j}\omega\mathcal{L}\dot{\Phi} + \mathrm{j}\frac{1}{\omega C}\dot{\Phi} \tag{6}$$

where ω is the angular frequency.

According to the magnetoelectric power law [20], the active power of the magnetic circuit can be obtained:

$$P = P_{\mathcal{L}} + P_C = \omega\left(\mathcal{X}_{\mathcal{L}}\left\|\dot{\Phi}\right\|^2 + \mathcal{X}_C\left\|\dot{\Phi}\right\|^2\right) = \omega^2\frac{N^2}{R}\left\|\dot{\Phi}\right\|^2 + \omega\frac{h\sin\gamma}{\mu A}\left\|\dot{\Phi}\right\|^2 \tag{7}$$

where R is the resistance of the magductance component, γ is the hysteresis angle of the hysteretance component [21], h is the height of the hysteretance component, and A is the cross-sectional area of the hysteretance component. Eq. (7) provides a new analytical model to calculate the loss in magnetic circuit, consisting of two parts: one part is $\mathcal{P}_{\mathcal{L}}$ on magductance component, corresponding to the eddy current loss. The other one is $\mathcal{P}_C$ on hysteretance component, corresponding to the hysteresis loss.

The reactive power of the magnetic circuit is:

$$Q = \omega\mathcal{R}\left\|\dot{\Phi}\right\|^2 \tag{8}$$

For the rectangular section shown in Fig. 2, we combine vector magnetic circuit theory and finite Fourier transform method [22]. Considering the spatial distribution of magnetic field strength and induced current density J, the white rectangular section in Fig. 2 is composed of different orange rectangular magnetic circuit components stacked together. These magnetic circuits are independent of each other. For each magnetic circuit element, the reluctance $\mathcal{R}_{mn}$ in each circuit represents the obstruction effect on the magnetic circuit, the magductance $\mathcal{L}_{mn}$ represents the eddy current effect in the magnetic circuit, and the hysteretance C_{mn} represents the hysteresis loss in the magnetic circuit.

The analytical expressions for parameters of each magnetic circuit component are given as:

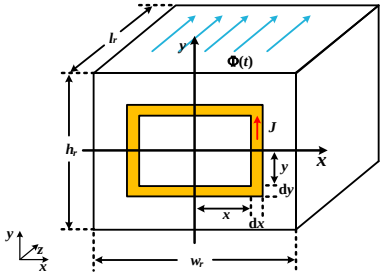

Fig. 2 Mathematical model of rectangular cross-section magnetic circuit

$$\mathcal{R}_{mn} = \frac{\pi^4 m^2 n^2 l_r}{64\mu w_r h_r} \tag{9}$$

$$\mathcal{L}_{mn} = \frac{\pi^4 m^2 n^2 \sigma l_r}{64 w_r h_r\left(\frac{m^2\pi^2}{w_r^2} + \frac{n^2\pi^2}{h_r^2}\right)} \tag{10}$$

$$C_{mn} = \frac{64\mu w_r h_r}{\omega\sin\gamma\pi^4 m^2 n^2 l_r} \tag{11}$$

where w_r is the width of a rectangular cross-section, h_r is the height of the rectangular section, l_r is the length of the rectangular section, σ is the conductivity of the magnetic core, m is an odd number, and n is an integer.

Given the specific geometric shape, conductivity, and permeability of the magnetic circuit, the magnetic circuit parameters can be calculated using Eqs. (9)-(11). In consequence, the core loss can be calculated as:

$$P = \sum_{\substack{n=\\1,2,3\ldots}}^{\infty}\sum_{\substack{m=\\1,3,5\ldots}}^{\infty}(P_{\mathcal{L}} + P_C) = \sum_{\substack{n=\\1,2,3\ldots}}^{\infty}\sum_{\substack{m=\\1,3,5\ldots}}^{\infty}(\omega^2\mathcal{L}_{mn}\left\|\dot{\Phi}_{mn}\right\|^2 + \frac{\left\|\dot{\Phi}_{mn}\right\|^2}{C_{mn}}) \tag{12}$$

In reference [21], we validated the effectiveness of the analytical model using silicon steel sheets. Due to space limitations, this article will not provide more details.

IV. Application Methods

Sections II and III presented the concept of vector magnetic circuit theory and analytical loss model. In practical applications, accurate calculation of magnetic circuit parameters is a new challenge. The literature [23] has identified various factors that influence magnetic core loss, including magnetic core material, size, magnetic density, frequency, and excitation type. However, the material manufacturers provide limited data, typically consisting of

fixed descriptions of loss curves and magnetic permeability change graphs with incomplete values over a wide range. Therefore, the loss calculations have been conducted by parameters fitting for magductance and hysteretance in Eq. (7), which is different from existing loss models.

A. The Impact of Frequency

The vector magnetic circuit theory can be employed in turn to derive the values of magductance and hysteretance, as follows:

$$P_v = k_e f^2 + k_h f \tag{13}$$

$$\mathcal{X}_{\mathcal{L}} = \frac{k_e f^2}{\omega\left\|\dot{\Phi}\right\|^2} = \frac{k_e f}{2\pi\left\|\dot{\Phi}\right\|^2} \tag{14}$$

$$\mathcal{X}_{C} = \frac{k_h f}{\omega\left\|\dot{\Phi}\right\|^2} = \frac{k_h}{2\pi\left\|\dot{\Phi}\right\|^2} \tag{15}$$

where P_v represents the volumetric loss of the magnetic circuit, k_h is the hysteresis loss coefficient, k_e is the eddy current loss coefficient, and f is the frequency. Using Eqs. (7), (12)-(15), we have derived the loss frequency relationship curve for 3E6 material exposed to sinusoidal excitation with a magnetic density amplitude of 0.1T at 25℃, as depicted in Fig. 3. Similarly, Fig. 4 displays the loss frequency relationship curve for N87 material under sinusoidal excitation with a magnetic density amplitude of 0.035T at 25℃. The "Pred_Volumetric_Loss" is the predicted total power loss, the "Pred_Hysteresis_Loss" is the predicted hysteresis loss, the "Pred_Eddycurrent_Loss" is the predicted eddy-current loss, and the "Competition Volumetric_Loss" is the total loss data provided by the competition organizer. The numerical values in the labels of the figures are arranged from left to right, which represent the predicted volume loss at each data point from low to high frequency, along with the percentage of error compared to the corresponding competition data.

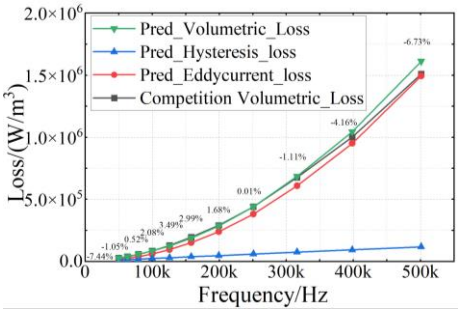

Fig. 3 The loss frequency relationship curve for 3E6 material exposed to sinusoidal excitation with a magnetic density amplitude of 0.1T at 25℃

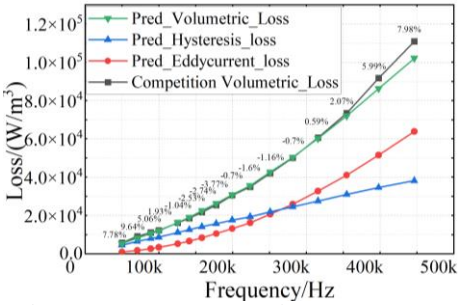

Fig. 4 The loss frequency relationship curve for N87 material exposed to sinusoidal excitation with a magnetic density amplitude of 0.035T at 25℃

The average values of errors shown in Figs. 3 and 4 are -0.89% and 2.88%, respectively. The effectiveness of our method within the wide frequency range under sinusoidal excitation has been proved. Furthermore, the method presented in this article allows for the determination of specific values of eddy current loss and hysteresis loss, as well as the patterns of frequency variation. For instance, comparing the eddy current losses in Figs. 3 and 4, we can see that the eddy current losses have always been the primary loss for 3E6 material. In contrast, for N87 material, as the frequency increases, the proportion of eddy current loss gradually exceeds hysteresis loss, highlighting that high conductivity magnetic core materials experience severe eddy current loss at high frequencies, while even low conductivity materials will experience more obvious eddy current loss at higher frequencies.

B. The Impact of Magnetic Density

Saturation has long been a significant source of nonlinearity in magnetic circuits [23]. When exposed to high frequency and intense magnetic fields, local saturation can occur within the magnetic core. Unfortunately, material manufacturers do not offer a quantitative assessment of the impact of this saturation, and only a limited amount of data can be obtained through experimental measurements. Our study addresses this issue by utilizing finite polynomials to fit changes in the eddy current coefficient and hysteresis coefficient with magnetic density amplitude. The specific form of our approach is outlined below:

$$k_e = a_1 B_m^{\ 3} + b_1 B_m^{\ 2} + c_1 B_m + d_1 \tag{16}$$

$$k_h = a_2 B_m^{\ 3} + b_2 B_m^{\ 2} + c_2 B_m + d_2 \tag{17}$$

where B_m is the amplitude of the sine wave excitation, and a_1, a_2, b_1, b_2, c_1, c_2, d_1, d_2 are the fitting parameters. By utilizing Eqs. (16)-(17) in conjunction with Eqs. (13)-(15), we are able to derive the magnetic circuit parameters for various levels of magnetic flux density. This process enables us to create a correlation curve between loss, frequency, and magnetic density for N87 material under sine wave excitation at 25 ℃, as shown in Fig. 5.

It should be mentioned that the aforementioned method can be used to determine the magnetic circuit parameters for different temperature states using Eqs. (13)-(17). Due to space limitations, we only show the case of 25 ℃ here.

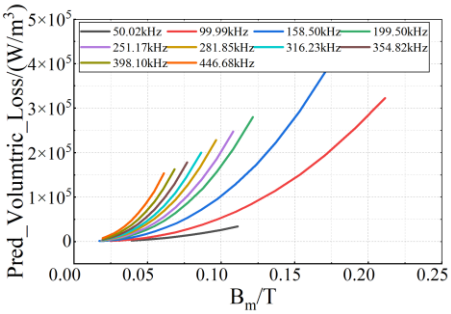

Fig. 5 The correlation curve between loss, frequency, and magnetic density for N87 material under sine wave excitation at a temperature of 25 ℃

The average discrepancy between the predicted and experimental loss data on N87 material with sine wave excitation at 25℃ is 4.67%. Fig. 5 reveals that the loss also

increases gradually with an increase in magnetic density under the same frequency. Similarly, an increase in frequency also leads to a gradual increase in loss under the same magnetic density. If there are sufficient data available, a three-dimensional surface figure can be formed by combining the loss, frequency, and magnetic density.

C. The Impact of Excitation Type

In practical applications with high frequencies, triangular and trapezoidal wave excitations are commonly utilized. To address the inaccuracies in traditional Steinmetz mode calculations under these waveforms, some scholars have proposed the iGSE (improved general Steinmetz equations) [9] and i^{2}GSE (improved-improved general Steinmetz equations) [11] models using empirical formula methods in recent years. Differently, this article proposes a new analytical loss modeling method by using vector magnetic circuit theory.

Previously, we obtained the magnetic circuit parameters under sinusoidal excitations at varying frequencies and magnetic densities. In signal processing, Fourier decomposition is often used to transform arbitrary waveform into a superposition of sine waves with different frequencies. Some scholars have attempted to use this method for magnetic circuit analysis before, but their results have not been satisfactory [8], [24-25]. From a vector magnetic circuit perspective, we believe that signals can be decomposed through Fourier transform, but magnetic circuit parameters cannot. Additionally, an arbitrary waveform cannot produce multiple magnetic permeabilities in a definite working state of the magnetic circuit. Therefore, the hysteresis coefficient k_h and eddy-current coefficient k_e under any excitation are primarily related to the peak value of the current excitation, which can be expressed as magnetic circuit parameters:

$$k_e = a_1 B_{peak}{}^3 + b_1 B_{peak}{}^2 + c_1 B_{peak} + d_1 \tag{18}$$

$$k_h = a_2 B_{peak}{}^3 + b_2 B_{peak}{}^2 + c_2 B_{peak} + d_2 \tag{19}$$

$$\mathcal{X}_{\mathcal{L}_n} = \frac{k_e f_n{}^2}{\omega_n \left\|\dot{\Phi}\right\|^2} = \frac{k_e f_n}{2\pi \left\|\dot{\Phi}\right\|^2} \tag{20}$$

$$\mathcal{X}_C = \frac{k_h f_n}{\omega_n \left\|\dot{\Phi}\right\|^2} = \frac{k_h}{2\pi \left\|\dot{\Phi}\right\|^2} \tag{21}$$

where B_{peak} is the magnetic density peak of arbitrary waveform, and the quantities with n are the magnetic circuit parameters corresponding to the nth harmonic after Fourier decomposition.

Eqs. (20) and (21) demonstrate that when various sine waves with different amplitudes and frequencies are obtained through Fourier decomposition, the magnetic circuit will generate magductance corresponding to different frequencies. Eqs. (20) and (21) also show that the hysteretance of the magnetic circuit is only related to the excitation's B_{peak} value. In summary, the eddy-current loss can be superimposed while the hysteresis loss cannot be superimposed. This judgement agrees with the physical characteristics of hysteresis loss and eddy current loss [26]. On the other hand, this part cannot be analyzed using the existing empirical formula methods.

By combining Eqs. (20), (21) and (7), we can obtain that the loss corresponding to arbitrary waveform excitation can be expressed as follows:

$$P_v = \sum_1^n \omega_n (\mathcal{X}_{\mathcal{L}_n} + \mathcal{X}_C) \left\|\dot{\Phi}\right\|^2 \tag{22}$$

As per the computation prescribed in Eq. (22), the error distribution histograms of 3E6 and N87 materials were obtained under arbitrary excitation waveforms at multiple magnetic-density points and multiple frequency points at a standard temperature of 25 ℃, as shown in Figs. 6 and 7.

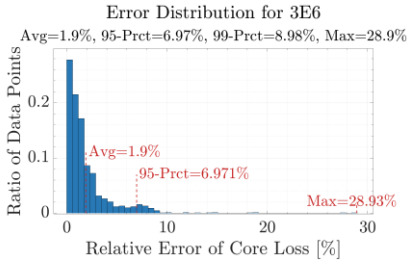

Fig. 6 The error distribution histograms of 3E6 materials were obtained under arbitrary waveform excitation at multiple magnetic density points and multiple frequency points at a standard temperature of 25 ℃

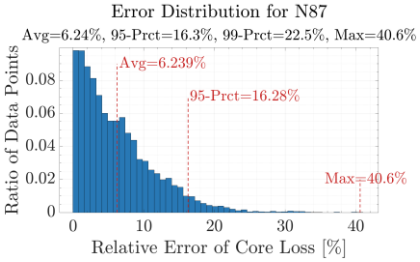

Fig. 7 The error distribution histograms of N87 materials were obtained under arbitrary waveform excitation at multiple magnetic density points and multiple frequency points at a standard temperature of 25 ℃

It can be seen that the error of 95% of the data for material 3E6 is less than 6.972%, while the error for N87 material is 16.28% for the same percentage. After comparing Figs. 6 and 7, the average error, 95-prct error, and maximum error for N87 material are all higher than those of 3E6 material. Based on material properties, the most significant difference between these two materials is their conductivity, which varies by 100 times. Additionally, the comparison between frequency in Figs. 3 and 4 reveals a notable difference in the proportion of eddy current losses in the total losses of the two materials. This raises questions about the accuracy of the current algorithm in materials with low eddy current losses and the source of data with significant errors in the two materials. To answer these questions, we conducted further research.

Through our analysis of maximum error values, it was discovered that the N87 material experiences a loss four times greater under 80% duty cycle triangular wave excitation in comparison to 60% duty cycle triangular wave excitation. This difference is illustrated in Fig. 8, which depicts two types of triangular waves with equivalent frequency and magnetic density peak sizes. On the other hand, the 3E6 material only experiences a 20% difference under the same conditions.

The duty cycles of the two types of excitation waveforms are different, which are 60% and 80% respectively. But it is the difference in dB/dt values that results in the difference in hysteresis loss. As explained in [26], the hysteresis loss is caused by rotational friction of magnetic domains. This means that the faster the rotation speed of magnetic domain is, and

the greater the hysteresis loss is. As a result, the materials like N87 having a significant proportion of hysteresis loss, are more affected by d*B*/d*t*. Currently, this article is still in the stage of qualitatively analyzing the impact of d*B*/d*t* on hysteresis loss. Our next step is to study how we can quantitatively consider this impact with our method.

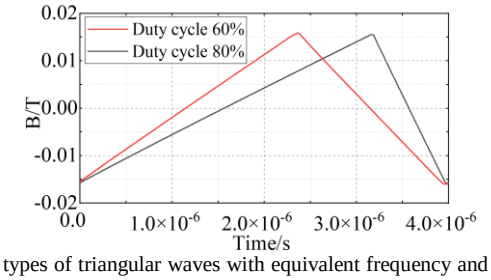

Fig. 8 Two types of triangular waves with equivalent frequency and magnetic density peak sizes.

V. Competition Contents

According to the methodology elucidated in this article, with regard to the final materials of A, B, C, D and E that were provided in the competition, we derived five distinct error distribution histograms from the training dataset. These histograms are graphically displayed in Fig. 9.

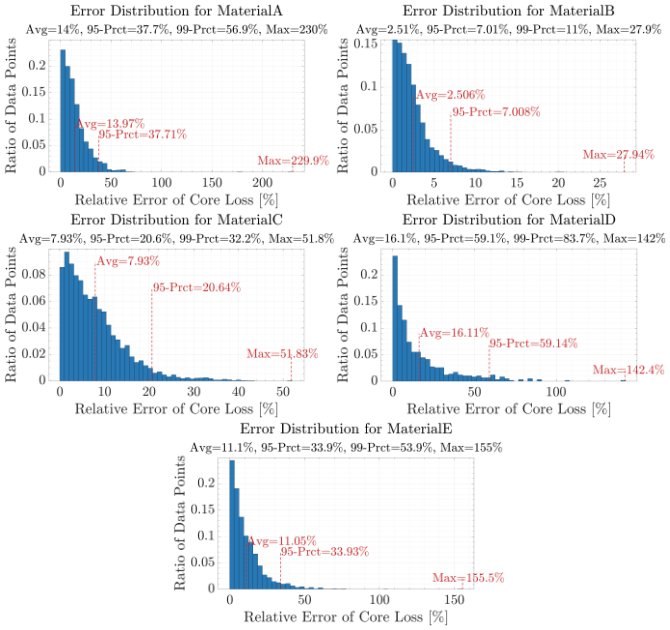

Fig. 9 The error distribution histograms of materials A, B, C, D and E from the training data.

The model size and numbers of parameters for each material (A, B, C, D, and E) are shown in Table I.

TABLE I
THE NUMBERS OF PARAMETERS FOR EACH OF THE MATERIAL

Material	A	B	C	D	E
Numbers of parameters	81	56	61	23	53
Model size (Byte)	5125	4421	4542	3255	4404

The statistical table of data points used for training and testing is shown in Table II.

TABLE II
THE AMOUNT OF TRAINING AND TESTING DATA

Material	A	B	C	D	E
Training data	2432 (101/69 4/1637)	7400 (364/225 3/4783)	5357 (215/167 9/3463)	580 (145/400/ 35)	2013 (57/667/ 1289)
Testing data	7651 (334/21 74/513)	3172 (147/980/ 2045)	5357 (212/175 4/3394)	7299 (61/2247/ 4991)	3738 (107/120 5/2426)

(The numbers in brackets denote the number of data points for sinusoidal waves, triangular waves, and trapezoidal waves, respectively.)

Based on our analysis in Fig. 9, the model is more effective for material B than material D. There are three sources of errors that we've identified:

1. The data used to train material B is more adequate than the data used to train material D. The results in more accurate curve fitting of eddy current loss and hysteresis loss with magnetic density and frequency.

2. The proportion of sine wave data used in the training is very small compared to other waveforms like triangular and trapezoidal waves. Although we can calculate the excitation of some other waveforms through Fourier decomposition, there is still a lack of quantitative research for excitation with large d*B*/d*t*.

3. For the final 5 materials, our model is relatively accurate in predicting materials with a high proportion of eddy current losses. Therefore, we can infer that material B has the highest conductivity among the 5 materials, while material D has a relatively small conductivity among the 5 materials.

VI. Conclusion

The vector magnetic circuit theory provides a different prospective and modeling method for predicting power loss in magnetic circuits. Different from existing core loss modeling methods, the proposed vector magnetic circuit based modeling method offers the following features: Firstly, it presents an analytical solution to evaluate the eddy-current loss and the hysteresis loss for magnetic cores by introducing the concepts of magductance and hysteretance in magnetic circuits. Given the complete geometrical and physical parameters of magnetic cores, the magductance and hysteretance parameters can be directly calculated, which can predict the eddy-current loss and hysteresis loss with magnetoelectric power law. Secondly, the proposed method offers the clear physical descriptions, i.e., magductance and hysteretance for eddy-current loss and hysteresis loss, which are not available by the existing loss modeling methods with abstract loss coefficients. Thirdly, the proposed method provides a new expression form for core loss. Even the material parameters are not available, the nonlinear fitting can be employed to evaluate the loss parameters and thus derive the loss model effectively.

Last but not least, we are very grateful to the organizers for organizing such a competition in 100-year honor of Prof. Charles P. Steinmetz (1865-1923). We hope that the vector magnetic circuit theory can provide an effective analytical modeling method for analyzing and calculating core losses.

REFERENCES

[1] D. C. Jiles, "Frequency dependence of hysteresis curves in conducting magnetic materials," *J. Appl. Phys.*, vol. 76, pp. 5849–5855 1994.

[2] A. Krings and J. Soulard, "Overview and comparison of iron loss models for electrical machines," *J. Elect. Eng.*, vol. 10, pp. 162–169, 2010.

[3] G. Bertotti, "General properties of power loss in soft magnetic material," *IEEE Trans. Magn.*, vol. 24, no. 1, pp. 621–630, Jan. 1988.

[4] D. C. Jiles and D. L. Atherton, "Theory of ferromagnetic hysteresis," *Magn.Magn. Mater*., vol. 61, pp. 48–60, 1986.

[5] A. Courtay, *The Preisach Model*. Austin, TX, USA: Analogy Inc., 1999.

[6] S. Barg, K. Ammous, H. Mejbri, and A. Ammous, "An improved empirical formulation for magnetic core losses estimation under nonsinusoidal induction", *IEEE Trans. on Power Electron.*, vol. 32, no. 3, pp. 2146-2154, Mar. 2017.

[7] C. P. Steinmetz, "On the law of hysteresis", *Proc. IEEE*, vol. 9, no. 2, pp. 3-64, 1892.

[8] J. Reinert, A. Brockmeyer, and R. W. De Doncker, "Calculations of losses in ferro- and ferromagnetic materials based on modified Steinmetz equation," *IEEE Trans. Ind. Appl*., vol. 37, no. 4, pp. 1055–1061, Jul./Aug. 2001.

[9] J. Li, T. Abdallah, and C. R. Sullivan, "Improved calculation of core loss with nonsinusoidal waveforms," in *Proc. IEEE Annu. Meeting Ind. Appl. Soc*., 2001, pp. 2203–2210.

[10] K. Venkatachalam, C. R. Sullivan, T. Abdallah, and H. Tacca, "Accurate prediction of ferrite core loss with non-sinusoidal waveforms using only Steinmetz parameters," in *Proc. IEEE Workshop Comput. Power Electron.*, 2002, pp. 36–41.

[11] J. Muhlethaler, J. Biela, J. W. Kolar, and A. Ecklebe, "Improved core-loss calculation for magnetic components employed in power electronic systems," *IEEE Trans. Power Electron.*, vol. 27, no. 2, pp. 964–973, Feb. 2012.

[12] H. Li, D. Serrano, S. Wang, T. Guillod, M. Luo, and M. Chen, "Predicting the B-H loops of power magnetics with transformer-based encoder-projector-decoder neural network architecture," in *Proc. IEEE Appl. Power Electron. Conf. Expo*., 2023, pp. 1543–1550.

[13] M. Chen, H. Li, D. Serrano, and S. Wang, "MagNet-AI: Neural network as datasheet for magnetics modeling and material recommendation," techRxiv, Preprint, 2023. [Online]. Available: https://doi.org/10.36227/techrxiv.22726115.v1.

[14] T. Guillod, P. Papamanolis, and J. W. Kolar, "Artificial neural network (ANN) based fast and accurate inductor modeling and design," *IEEE Open J. Power Electron.*, vol. 1, pp. 284–299, 2020.

[15] MagNet 2023 Team. Princeton University. (2023, Apr. 7). *2023 PELS-Google-Tesla-Princeton MagNet Challenge*. [Online]. Available: http://www.princeton.edu/~minjie/magnet.html.

[16] E. Colin Cherry, "The duality between interlinked electric and magnetic circuits and the formation of transformer equivalent circuits," *Proc. Phys. Soc. B*, vol. 62, no. 2, pp. 101–111, Feb. 1949.

[17] Ion Boldea, "Linear electric machines drives, and MAGLEVs handbook", CRC Press, Taylor & Francis, New York, 2013.

[18] K. A. Macfadyen, "Vector permeability," *Proc. Inst. Elect. Engineers*, vol. 95, issue 85, pp. 63-64, Jan. 1948.

[19] Laithwaite E R., "Magnetic equivalent circuits for electrical machines", *Proc. Inst. Elect. Engineers*, vol. 114, no. 11, pp. 1805–1809, Nov. 1967.

[20] M. Cheng, W. Qin, X. Zhu and Z. Wang, "Magnetic-Inductance: Concept, Definition, and Applications," *IEEE Trans. on Power Electron.*, vol. 37, no. 10, pp. 12406-12414, Oct. 2022.

[21] W. Qin, M. Cheng, Z. Wang, Z. Ma, S. Zhu, M. Gu, X. Zhu, W. Hua, "Vector magnetic circuit theory and its preliminary applications," *Proc. CSEE*, 2023, https://link.cnki.net/urlid/11.2107.tm.20231103.1033.002.

[22] Stoll R L. *The analysis of eddy currents*. Oxford: Oxford University Press, 1974: 1-69.

[23] D. Serrano, H. Li, S. Wang, T. Guillod, M. Luo, etc., "Why MagNet: quantifying the complexity of modeling power magnetic material characteristics," *IEEE Trans. on Power Electron.*, vol. 38, no. 11, pp. 14292-14316, Nov. 2023.

[24] P. M. Gradzki, M. M. Jovanovic, and F. C. Lee, "Computer aided design for high-frequency power transformers," in *Proc. IEEE APEC'90*, 1990, pp. 336–343.

[25] R. Severns, "HF-core losses for nonsinusoidal waveforms," in *Proc. HFPC*, 1991, pp. 140–148.

[26] M. K. Kazimierczuk, *High-Frequency Magnetic Components*, 2rd ed., New York, USA: John Wiley & Sons. Ltd., 2014, pp. 383–411.